Front. Chem. Sci. Eng. 2022, 16(12): 1689−1699
https://doi.org/10.1007/s11705-022-2186-7

RESEARCH ARTICLE

Regulation of radicals by hydrogen-donor solvent in direct coal liquefaction

Wang Li, Wen-Ying Li (✉), Xing-Bao Wang, Jie Feng

State Key Laboratory of Clean and Efficient Coal Utilization, Taiyuan University of Technology, Taiyuan 030024, China

Abstract Radicals are important intermediates in direct coal liquefaction. Certain radicals can cause the cleavage of chemical bonds. At high temperatures, radical fragments can be produced by the splitting of large organic molecules, which can break strong chemical bonds through the induction pyrolysis of radicals. The reaction between the formation and annihilation of coal radical fragments and the effect of hydrogen-donor solvents on the radical fragments are discussed in lignite hydrogenolysis. Using the hydroxyl and ether bonds as indicators, the effects of different radicals on the cleavage of chemical bond were investigated employing density functional theory calculations and lignite hydrogenolysis experiments. Results showed that the adjustment of the coal radical fragments could be made by the addition of hydrogen-donor solvents. Results showed that the transition from coal radical fragment to H radical leads to the variation of product distribution. The synergistic mechanism of hydrogen supply and hydrogenolysis of hydrogen-donor solvent was proposed.

Keywords direct coal liquefaction, hydrogen-donor solvent, induced pyrolysis, radical mechanism, density functional theory calculations

1 Introduction

Since the early 20th century, direct coal liquefaction has dramatically progressed from laboratory to industrial-scale [1–3]. Aside from catalysts and hydrogen pressure, the hydrogen-donor solvent can remarkably increase the oil yield by inhibiting the condensation of the low rank coal hydrogenolysis [4–6]. In the industry, complex organic molecules such as polycyclic aromatic hydrocarbons dissolved in coal and their hydrogenated counterparts, served as the hydrogen source [7,8]. Niu et al. [9] investigated the direct coal liquefaction using tetralin as the hydrogen-donor solvent and other polyaromatic solvents (phenanthrene, pyrene, and fluoranthene) for coal dissolution without using a catalyst. In addition to dissolving and dispersing the coal particles, such polyaromatic solvents underwent hydrogenation to yield 9,10-dihydrophenanthrene, 4,5-dihydropyrene, and 1,2,3,10b-tetrahydrofluoranthene, all of which donated their hydrogen atoms effectively during the direct coal liquefaction. In additional studies [9], the same authors used the isotopic labeling method to analyze the source of hydrogen atoms. Without a catalyst, 80% of the hydrogen consumption was made from the hydrogen-donor solvent under non-isothermal conditions, whereas the hydrogen-donor solvent contributed 65% of the hydrogen consumption under isothermal conditions, implying that the solvent has a substantial role in the reaction results [10,11]. Similarly, if the ratio of hydrogen-donor solvent to coal was different, it would result in a difference in product distribution. Generally, increasing the proportion of hydrogen-donor solvent could increase the oil yield during the direct coal liquefaction [12]. When coal is being heated, radical fragments can be generated, which would condense if required amount of hydrogen is unavailable at the time. Thus, the presence of a hydrogen-donor solvent decreases the likelihood of condensation [12,13].

Radicals are crucial intermediates in the coal or lignin conversion [14–18]. These radicals have been shown to promote the breakdown of chemical bonds, called induced pyrolysis [19]. If the hydrogen-donor solvent is present, these radicals from coal pyrolysis are stabilized promptly, thereby weakening the induced pyrolysis. Therefore, the pyrolysis of alkyl benzene was dissociated into direct and induced pyrolysis, in the presence or absence of hydrogen-donor solvent, and the kinetics of both pyrolysis were calculated [19]. The induced pyrolysis of alkyl benzene will increase at higher

Received March 31, 2022; accepted May 12, 2022

E-mail: ying@tyut.edu.cn

temperatures. The main reason for this is that as temperature rises, so does the amounts of radicals produced by direct pyrolysis. However, for the simulation process that depends on the strength of chemical bonds for thermal decomposition, the simulation at low temperature is quite distinct from the actual transformation [20]. According to their calculation results, the induction effect may be more noticeable in the pyrolysis system of coal at low temperatures [21]. Induced pyrolysis was proposed yet, while the intricacies of its mechanism and that of the hydrogen-donor solvent, notably for coal hydrogenolysis, have not been thoroughly analyzed in previous studies. In recent years, Reax FF reactive force field has been used to simulate the coal conversion process, thus gradually clarifying the reaction mechanism [22]. However, the reactions among radicals formed during the thermal conversion are not well understood, particularly when the hydrogen-donor solvent is involved.

If tetralin is used as a hydrogen-donor solvent for the hydrogenolysis of coal, the bond energy of the C–H bond is relatively high compared to that of aliphatic carbon oxygen bond (C_{al}–O), making it challenging to break directly [23]. Researchers confirmed that radical fragmentation's energy barrier for extracting H from a hydrogen-donor solvent is minimal, as shown in Fig. S1 (cf. Electronic Supplementary Material, ESM) [7]. Once radicals remove one H atom from the hydrogen-donor solvent, it will become a hydrogen-donor-solvent radical. Thus, the participation of hydrogen-donor solvent may change the types of radicals in the system.

Most researchers considered that the conversion of hydrogen-donor solvent to hydrogen-donor-solvent radical was important for the reaction [12]. If the hydrogen supplying mechanism is followed as Fig. S1, the energy barrier is easier to overcome than C–H direct cleavage [24]. Nonetheless, there are remarkable discrepancies between different hydrogen-donor solvents during the hydrogenolysis of coal or some model compounds [25]. These differences may cause by the abstraction from hydrogen-donor solvent and the sequence dehydrogenation. As a result, the influence on the coal conversion of hydrogen-donor-solvent radical formed after the hydrogen supply procedure of hydrogen-donor solvent needs to be evaluated. Hydrogen-donor-solvent radical is a radical that needs to be successive dehydrogenated or combined with other radicals to be stable. In other words, since radical fragments are produced during the coal conversion, these radical fragments are annihilated by hydrogen-donor solvent to produce a new radical hydrogen-donor-solvent radical. The alterations greatly influence the chemical bond cleavage induced by these radical species. Suppose the hydrogen-donor-solvent radical comes in contact with the radicals produced by coal pyrolysis. In that case, they are more likely to bind together, a process that does not need to overcome an energy barrier. However, this combination increases the product's molecular weight, which is detrimental to oil yields. Moreover, this process only caused by the combination of radicals is challenging to regulate. To avoid this situation, the proportion of hydrogen-donor solvent is frequently increased. Since hydrogen-donor-solvent radical's ability to bind to radicals is reduced, it must undergo unimolecular reactions to become stable. The H radicals formed by the hydrogen-donor-solvent radicals unimolecular processed can participate in the radical-induced cleavage triggered by H radicals, affecting the direct coal liquefaction. The possibility of hydrogenolysis by H radicals depends on the reaction conditions, which determines the hydrogen utilization and product distribution efficiency [1,26]. These processes are all caused by the participation of hydrogen-donor solvents. Still, the mechanism of hydrogen supplying and hydrogenolysis has not been thoroughly elaborated, particularly the impact of these radicals on the cleavage of strong chemical bonds. Therefore, this research will investigate the role of radicals in the entire process using density functional theory (DFT) calculation and hydrogenolysis of coal.

In the organic structure of coal, there are many kinds of chemical bonds, including the C_{al}–O, which is relatively weak [27]. Also, the hydrogenolysis of the ether bond will produce hydroxyl groups, which will be easier to distinguish. For example, benzyl phenyl ethers are often used as model compounds to convert low-rank coal or lignin [28]. C_{al}–O breaks into benzyl and phenoxy radicals, which are stabilized by hydrogen to form phenol or toluene [29]. However, radicals will affect the produced phenol in the reaction, reducing the yield of phenolic compounds. These coal-based model compounds are more sensitive to radicals in the transformation process. As a result, during the hydrogenolysis of lignite, the influence of hydrogen-donor solvent on chemical bonds was examined using the transformation process of the C–O–C bond as an example from the perspective of adjusting radicals.

These findings are crucial for clarifying the hydrogen supplying mechanism in the direct coal liquefaction and preparing phenolic compounds from lignin or low-rank coal hydrogenolysis.

2 Experimental

2.1 Chemical reagent

HulunBuir lignite from China, low-rank coal to be easily liquefied, was chosen as the subject of study and dried at 120 °C for 12 h (grain diameters are between 0.106 mm and 0.150 mm, same diameter range with most research work). Table 1 shows the results of proximate and ultimate analyses of lignite. Tetralin (99.5%) and

Table 1 Proximate and ultimate analysis of lignite (wt %) [30]

Proximate analysis [a]				Ultimate analysis (dry ash-free) [b]				
M_{ad}	A_d	V_d	FC_d	C	H	N	S	O
11.44	14.80	37.35	47.84	68.65	4.97	0.97	0.32	23.63

a) M = moisture; A = ash; V = volatiles; FC = fixed carbon; ad = air dry; d = dry; b) C, H, N, and S were obtained directly by the CHNS model and O content was obtained by O model.

1-methylnaphthalene (98%) were purchased from Aladdin in China, whereas *n*-hexane (97%) was obtained from Macklin in China.

2.2 DFT calculations of the chemical bond dissociation enthalpy (BDE)

DFT was employed to calculate the reaction energy barrier, by software Gaussian 09 [31]. Geometry optimizations and frequency calculations were performed at (U)M06-2X/def2tzvp level of theory using Grimme's DFT-D3 dispersion correction [32]. The final energies were further improved by computing single-point energy at the B2PLYP/def2TZVPP level on the optimized geometries [7,33], and Grimme's DFT-D3 dispersion correction was used with Becke–Johnson damping function. The liquid phase environment of the direct coal liquefaction was accessed using tetralin (permittivity (ε) = 2.77) in the SMD solvation model [24]. A temperature correction was incorporated with the usual direct coal liquefaction temperature of 400 or 450 °C. To scan the transition states and confirm that optimum transition states were coupled to the reactants and product, an intrinsic reaction coordinate analysis was applied.

The enthalpy values were calculated using the previous method [34]. The chemical BDE values were calculated with the following Eqs. (1) and (2):

$$\mathrm{BDE(A-B)} = [\mathrm{H(A\cdot)} + \mathrm{H(B\cdot)}] - \mathrm{H(A-B)}, \quad (1)$$

where H(A·), H(B·), and H(A–B) are the enthalpies of the cleaved radical species A· and B· and the model compound A–B, respectively. The free energy barrier (ΔG) for the activation between reactant and transition state is defined as:

$$\Delta G = G_{\mathrm{TS}} - G_{\mathrm{reactant}}, \quad (2)$$

where G_{TS} and G_{reactant} represent the energies of transition state and reactant (free energy + zero-point energy correction by Gaussian 09), respectively. All energies are given in kJ·mol^{-1} [27].

2.3 Hydrogenolysis of coal

The lignite was initially disseminated well in the tetralin before being poured into a quartz tube (no catalysis was used). The diagram of the reaction device is shown in Figure S2 (cf. ESM). The quartz tube was inserted into the autoclave reactor with 50 mL capacity (Anhui Kemi Machinery Technology Co., Ltd., China). The reactor was purged using H_2 (2–3 MPa). Before starting the experiments, a leak test was conducted for the reaction device.

Temperature and pressure were recorded before (T_1 and P_1) and after the reaction (T_2 and P_2). The temperature of the reactor program was reached at a heating rate of 5 °C·min^{-1}. After attaining the set temperature, the heating was stopped, and the product was immediately cooled to room temperature with cold water before it was collected for analysis.

Previous results have shown that 400 °C was one of the critical points for the hydrogenolysis of lignite [26]. So, the hydrogenolysis at 400 °C was investigated in this study, set as Series 1. The products at the ratio of tetralin/coal = 0, 2, 4, 6, 8, and 16 were analyzed separately, and the corresponding samples were labeled as 1–0, 1–2, 1–4, 1–6, 1–8, and 1–16. An obvious condensation reaction occurred when the temperature was set at 450 °C for 40 min [35]. Under such reaction conditions, the hydrogenolysis of lignite under different ratios of tetralin/coal was analyzed, including 0, 2, 4, 6, 8, and 16, marked as Series 2, and the corresponding samples were labeled 2–0, 2–2, 2–4, 2–6, 2–8, and 2–16, respectively. To reduce the influence of solvent dispersive coal on transformation, when the ratio of tetralin to coal was less than 4, 1-methylnaphthalene was used as a solvent supplement. Tetralin/coal = 0 (coal: tetralin:1-methylnaphthalene = 1:0:4); tetralin/coal = 2 (coal:tetralin:1-methylnaphthalene = 1:2:2); tetralin/coal = 4 (coal:tetralin:1-methylnaphthalene = 1:4:0).

2.4 Separation and quantitively analysis of product

2.4.1 Separation of products after lignite hydrogenolysis

Soxhlet extraction was used to separate the mixture (including the liquid and solid products). Initially, 100 mL of *n*-hexane was used as the extraction solvent, and the extraction time was 24 h at 70 °C (water bath temperature). The filter was dried for 12 h to ensure the constant weight, and the obtained soluble substance was named oil, and the *n*-hexane insoluble substance was termed NHI. The mass percent values of liquefaction products were calculated using Eqs. (3) to (6):

$$\text{Yield of water}: Y_{\mathrm{w}} = a \times \frac{m_{\mathrm{mixture}}}{m_{\mathrm{coal}}} \times 100\%, \quad (3)$$

$$\text{Yield of oil}: Y_{\mathrm{O}} = \frac{m_1 - m_{\mathrm{THN}}}{m_{\mathrm{coal}}} \times 100\%, \quad (4)$$

$$\text{Yield of NHI}: Y_{\text{NHI}} = \frac{m_2}{m_{\text{coal}}} \times 100\%, \quad (5)$$

$$\text{Yield of gas}: Y_{\text{G}} = \frac{100V_1}{22.4m_{\text{coal}}} \times \frac{P_2 + 0.1}{0.1} \times \frac{273.15}{T_2 + 273.15} \times \sum R_i\mu_i \times 100\%, \quad (6)$$

where m_1: soluble mass of *n*-hexane (g); m_{THN}: mass of solvent in the extracted sample (g); m_2: mass of insoluble in *n*-hexane (g); m_{coal}: lignite mass (g); a: water content of the sample tested by Calfius moisture analysis instrument; m_{mixture}: mass of solid–liquid mixture in the lining after reaction (g); V_1: volume of gas after reaction (0.05 L); P_2: post-reaction pressure (MPa); T_2: post-reaction temperature (°C); R_i: volume percentage of each gas component (including H_2, CH_4, CO, and CO_2); μ_i: molecular weight of corresponding gas. And the product distribution is shown in Fig. S3 (cf. ESM).

2.4.2 Analytical techniques for gas and oil products

Coal was liquefied into several products, including solid, liquid, and gaseous products. The product yield was based on dry ash-free basis.

Gas: using gas chromatography (GC-950, Haixin, Shanghai, China), the gaseous products were identified as H_2, CH_4, CO, and CO_2 and quantified using an external standard method.

Oil: *n*-hexane-extracted oil product was diluted with dichloromethane before the estimation using 2D gas chromatography (Shimazu GC-2010 plus, GC × GC-MS/FID via ZOEX, Japan) comprising the first column as DB-1 (15 m × 0.25 mm × 0.25 μm) and the second column as BPX-50 (2 m × 0.1 mm × 0.1 μm) using two detectors such as mass spectroscopy (GCMS-QP2020) and flame ionization. The inlet temperature was 280 °C. The initial temperature of the GC program was 50 °C, and increased to 140 °C at a rate of 3 °C·min^{-1} and maintained at 140 °C for 2 min. The temperature was further increased to 190 °C at a rate of 2 °C·min^{-1} and then raised to 280 °C at a rate of 3 °C·min^{-1}, and kept at 280 °C for 2 min.

Water: the water content was tested by a Calfius moisture analysis instrument (915KF Ti-Touch of Metrohm, Switzerland).

2.4.3 Characterization of oxygen-containing functional groups

The oxygen-containing functional groups were investigated by Bruker TENSOR 27 Fourier transform infrared spectroscopy (FTIR, Germany) in the chosen range (600–4000 cm^{-1}) with a resolution of 2 cm^{-1}. The KBr disks were prepared in a 1:180 (sample: KBr) sampling ratio for the analysis. The observed characteristic peaks used for the absorbance [36] were 2925 (aliphatic C–H bond, C_{al}–H), 3030 (aromatical C–H bond, C_{ar}–H) and 1100 cm^{-1} (C–O–C). The absorbance of the desired peak was calculated using the following formula: $I_{\text{C–O–C}} = A_{1100}$, $I_{C_{ar}-H} = A_{3030}$, $I_{C_{al}-H} = A_{2925}$.

2.4.4 Electron paramagnetic resonance (EPR) spectroscopy for radical analysis

The radicals were investigated by EPR performed on the EMXplus-9.5/12 (Bruker, Germany) instrument. Before the analysis, the samples were carefully packed inside the capillary column of 2 cm in length.

3 Results and discussion

3.1 Formation of H radicals

For the hydrogenolysis of coal, the pyrolysis of large organic structures to generate small radical fragments is the first step [1,24]. However, we have discussed in the introduction section that the types of radicals changed after the participation of hydrogen-donor solvent. In other words, coal radical fragments mainly extract H from tetralin to be stabilized in the absence of a catalyst, as shown in Fig. S1. The extraction of H atom from tetralin by coal radical fragments is the second step, rather than coal radical fragments combining with H atoms produced by the self-dissociation of the C–H bond of tetralin. However, tetralin was converted to tetralin radicals after a hydrogen atom was extracted, also a radical fragment. If the hydrogen-donor-solvent radical meets the other radical, they will quickly bond together without overcoming an energy barrier. However, the continuous supply of hydrogen by the hydrogen-donor-solvent radicals to form naphthalene from tetralin suggests that they may not have encountered other radicals. There is the possibility of self-decomposition for the hydrogen-donor-solvent radical's stability requirement. The possible route of continued dehydrogenation of tetralin radicals by DFT calculation is shown in Fig. 1.

The above results indicate that the β C–H bond energy was remarkably reduced when the first hydrogen was removed by the hydrogen-donor solvent. The bond

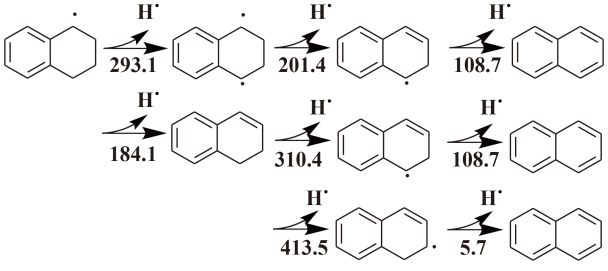

Fig. 1 Tetralin radical dehydrogenation (BDE, kJ·mol^{-1}).

energy of 184.1 kJ·mol^{-1} implies that the β C–H bond was easily broken during the hydrogenolysis of lignite, as shown in Fig. 1. When alkylbenzene was pyrolyzed, no H_2 was produced; however, when tetralin was added, H_2 was formed in a different proportion [19]. As a result, alkylbenzene with more extensive thermal cracking produced more H_2 [19]. That was also confirmed by a process that occurred for 9,10-dihydroanthracene and 9,10-dihydrophenanthrene. The BDE of C–H bond in 9,10-dihydroanthracene radical and 9,10-dihydrophenanthrene are 177.5 and 126.3 kJ·mol^{-1}, respectively, as shown in Fig. S4 (cf. ESM).

3.2 Induced pyrolysis of C_{al}–O of benzyl phenyl ether by radicals

There are mainly two kinds of radicals in this article to discuss. One is H radical; another is benzyl radical, used as a coal radical.

3.2.1 Induced pyrolysis initiated by benzyl radicals

The BDE of the C_{al}–O in benzyl phenyl ether is 231.5 kJ·mol^{-1} [26]. When the C_{al}–O of benzyl phenyl ether is broken, benzyl and phenoxy radicals are produced [37]. Suppose the two radicals are not stabilized in time, the benzyl radicals will activate the C_{al}–O of the benzyl phenyl ether, stretching the bond length when benzyl radicals closed to the benzyl phenyl ether according to Gaussian 09. The approximate free energy barrier to overcome is 335.4 kJ·mol^{-1} (450 °C), as shown in Fig. 2.

With the addition of hydrogen-donor solvent, benzyl and phenoxy radicals formed by the dissociation of benzyl phenyl ether were immediately annihilated, weakening the induced pyrolysis by coal radical fragments and completely inhibiting the conversion. However, as mentioned above, the presence of hydrogen-donor solvent can produce H radicals. Therefore, as the proportion of hydrogen-donor solvent increased, so did the concentration of H radicals. Beyond that, the induction process of the C_{al}–O under the influence of H radicals should be thoroughly investigated.

3.2.2 Induced pyrolysis initiated by H radicals

When the H radicals approached the benzyl phenyl ether, the main direction of attack was the O atom [26]. The DFT calculations show that the H radicals must overcome the energy barrier of 174.7 kJ·mol^{-1}, as indicated in Fig. 3. The energy barrier required was lower than that of benzyl radicals' induction (Fig. 2**)**. That meant benzyl phenyl ether dissociation was easier in the presence of H radicals (174.7 < 335.4 kJ·mol^{-1}, 450 °C), compared the benzyl radicals.

However, for the induced pyrolysis of H radicals, relevant studies suggested that active hydrogen species started saturating the aromatic ring by attacking $C_{\alpha(\beta)}$ but could not continue to hydrogenate to fully saturated products because of the limited concentration of active hydrogen [26]. In a similar study, the dissociation of the 4–O–5 (diphenyl ether was used as the model compound) was analyzed, and the hydrogenolysis of aromatical C–O bond (C_{ar}–O) was discovered to be primarily due to two steps: first, the aromatic was hydrogenated by one hydrogen atom, followed by its cracking into benzene and phenoxy radicals [38]. If the concentration of the H radical is very high, the benzene will be saturated. However, in this study, the source of H radicals was the reactive radical fragments accompanying the hydrogen donating process, resulting in a limited number of H radicals. Therefore, hydrogenolysis is more likely to occur in this study. The exact H free radical induced-pyrolysis may also exist for benzyl phenyl ether, but regardless of the path, the existence of H radicals will play a role in promoting the cleavage of the C–O bond [26].

3.3 Induced pyrolysis of phenolic hydroxyl by radicals

3.3.1 Phenolic hydroxyl as a hydrogen-donor source to be abstracted H

In the case of benzyl radicals, hydrogen was stabilized timely. When benzyl radicals approached the phenol, phenolic hydroxyl was induced to undergo a hydrogen transfer, which was needed to overcome an energy barrier of 205.7 kJ·mol^{-1} (450 °C). This value is lower than the energy barrier in benzyl radicals abstracting H from tetralin (213.3 kJ·mol^{-1}, 450 °C), as shown in Fig. 4. However, due to the relatively large size of benzyl radicals, there was a large steric hindrance in the induction process so that it was difficult to induce the pyrolysis [21], and the occurrence of hydrogen abstraction by benzyl radicals was easier.

Compared with H from tetralin, H of the phenol hydroxyl is easily abstracted by radical fragments during

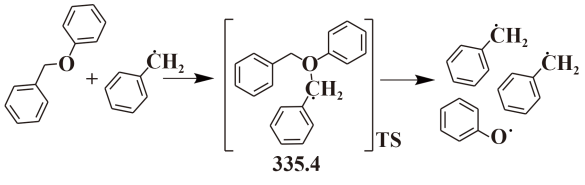

Fig. 2 Benzyl radical induced-pyrolysis of benzyl phenyl ether at 450 °C (TS energy barrier, kJ·mol^{-1}).

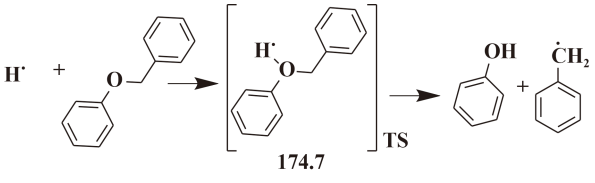

Fig. 3 Induced pyrolysis initiated by H radicals from the hydrogen-donor source at 450 °C (TS energy barrier, kJ·mol^{-1}).

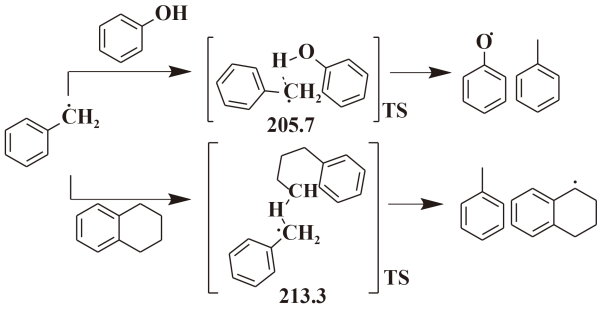

Fig. 4 H extraction from hydroxyl or tetralin initiated by benzyl radicals at 450 °C (TS energy barrier, kJ·mol^{-1}).

lignite pyrolysis. Therefore, it is deduced that if phenoxy radicals were not stabilized by hydrogen promptly, they would condense to form new C–O bonds that are hard to break [39].

During lignite pyrolysis, alkyl substitution products were heated to remove part of an alkyl group, among which methane was the main product. When methyl radicals approached phenolic hydroxyl groups, there were two activation pathways for phenolic hydroxyl groups, as shown in Fig. 5. In route 1, the O–H bond was activated in the same way as that of benzyl radicals, and hydrogen was transferred from phenol to radicals. In route 2, an O atom was induced to activate the C–O bond, causing phenol to remove the hydroxyl group.

Additionally, the methyl radicals were more likely to promote the dehydrogenation of phenolic hydroxyl into phenoxy radicals during the induced pyrolysis. The energy barrier was 149.4 kJ·mol^{-1}, as shown in Fig. 5.

3.3.2 Induced pyrolysis of the phenolic hydroxyl group by H radicals

If there were a lot of H radicals in the system, these H radicals would promote the breaking of C–OH into the water, presumably requiring an energy barrier of 236.1 kJ·mol^{-1}, as shown in Fig. 6.

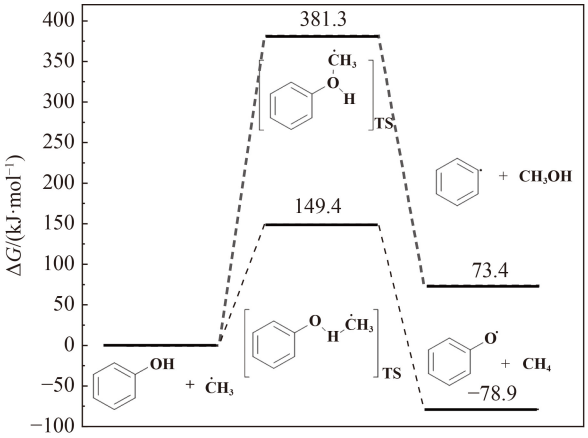

Fig. 5 Induced pyrolysis by CH_3 radicals at 450 °C.

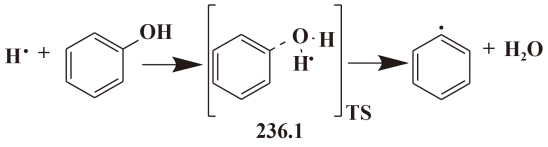

Fig. 6 Induced pyrolysis initiated by H radicals at 450 °C (TS energy barrier, kJ·mol^{-1}).

3.4 Effects of radicals on the formation of phenolic compounds

Based on the above analysis, the generation rule of phenolic compounds in lignite and the hydrogen supplying mechanism influence of hydrogen-donor solvent on the generation of pyrolysis were summarized in Fig. 7. Coal radical fragments were generated after the thermal decomposition of macromolecular organic compounds, and benzyl radicals were employed as the model radical index. It was found that benzyl radicals were more easily stabilized by hydrogen extraction from hydrogen-donor solvent. More benzyl radicals were

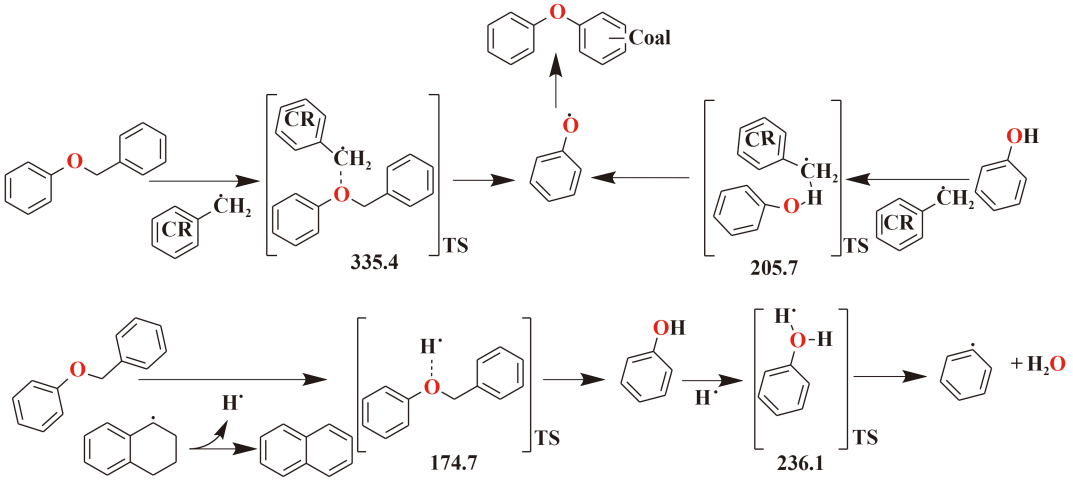

Fig. 7 Scheme of induced pyrolysis by radicals at 450 °C (CR: coal radical fragments; TS energy barrier, kJ·mol^{-1}).

stabilized when the amount of hydrogen-donor solvent was increased, thus blocking their participation in the induced pyrolysis. However, after the H of tetralin was abstracted by benzyl radicals, tetralin was transformed into an unstable tetralin radical. And the C–H BDE of tetralin radical was reduced to 184.1 kJ·mol^{-1}. The second H would be released quickly with the direct breakdown of C–H in tetralin radical. So, there will be H radicals transiently in an investigated system. While H radicals were partly used to stabilize coal radical fragments produced by pyrolysis, other H radicals decreased the energy barrier of breaking bonds. The tetralin proportion rose, and so did the induction of self-dissociating H radicals. However, because H radicals are so small, they are quickly annihilated, and their induction effect is limited.

3.5 Results of lignite hydrogenolysis

Given the radical mechanism mentioned above, the hydrogenolysis reaction of lignite under two conditions was analyzed [30]. One was at 400 °C, another was at 450 °C and lasted for 40 min. Materials balance and product distribution of the reaction are shown in Table S1 (cf. ESM) and Fig. S3. The overall mass balance was higher than 93 wt %. In addition, the yield of *n*-hexane insoluble products decreased with the increase in the tetralin proportion. For the reaction results of Series 1, when the m_{THN}/m_{coal} ratio was 2, the oil yield remained the same, while in Series 2, the oil yield had a peak value at the ratio of m_{THN}/m_{coal} was 4, as displayed in Fig. S3. Oil yield is primarily related to the occurrence of pyrolysis. In the absence of catalysis, pyrolysis is mainly influenced by thermodynamics. The participation of hydrogen-donor solvents promotes the stability of radicals. In this study, the tetralin radicals spontaneously generated H radicals, which can be used to induce pyrolysis. However, a free radical-induced reaction must be initiated by generating radicals. Therefore, when the m_{THN}/m_{coal} ratio was >2 in Series 1, the oil yield remained the same while that of Series 2 changed remarkably.

3.5.1 Relationship between phenolic hydroxyl groups and tetralin ratio

By comparing the ratio of phenol in Series 1 and 2 products with the yield of water (H_2O), it was observed that with the increase in the ratio of tetralin, the yield of phenolic compounds had a maximum value when the ratio of m_{THN}/m_{coal} was 4, as presented in Fig. 8. When the ratio of m_{THN} to m_{coal} was greater than 4, the water yield showed a trend of gradual increase, with phenols yield decreasing. This indicates that the de-hydroxylation reaction of phenol hydroxyl induced by H radicals occurs as the tetralin proportion increases.

Similarly, the results at 450 °C lasting for 40 min showed the same trend demonstrated in Fig. S5 (cf. ESM). When m_{THN}/m_{coal} was less than 4, it was mainly because the increase in the proportion of tetralin decreased the content of radical fragments from coal. The possibility of phenol as a hydrogen-donor source was reduced. Thus, the protection of the phenolic hydroxyl group was realized. When the ratio of m_{THN}/m_{coal} was greater than 4, the induction process of H radicals to –OH was promoted due to an increase in H radicals. Because of the existence of tetralin, the species of radicals in products changed from coal radical fragments to H radicals, as shown in Fig. 7.

3.5.2 Relationship between ether bonds and tetralin ratio

FTIR was employed to explore solid products from the hydrogenolysis of lignite at 400 °C, as shown in Fig. S6 (cf. ESM). The absorbance of C–O–C, C_{ar}–H, and C_{al}–H was analyzed and discussed in Fig. 9. The intensity of C_{al}–H/C_{ar}–H increased initially, then decreased as the proportion of tetralin increased, reaching its maximum value in the m_{THN}/m_{coal} range of 6 to 8. Increasing the proportion of tetralin before the peak point and the condensation process being effectively inhibited, the formation process of aliphatic C_{al}–H to aromatic C_{ar}–H can be reduced. When the proportion of tetralin increased, combined with the result of DFT calculations, the H radicals were generated. And part of the H radicals

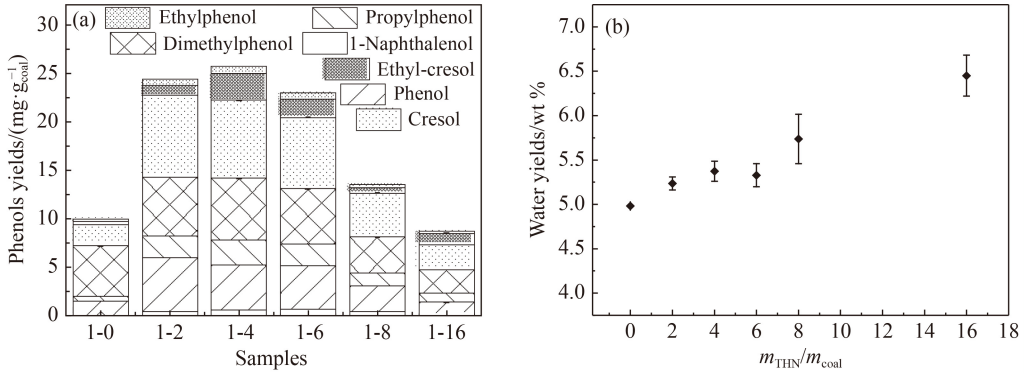

Fig. 8 (a) Variation of phenolic compounds and (b) water yields with different ratios of tetralin to coal at 400 °C and 6 MPa of H_2.

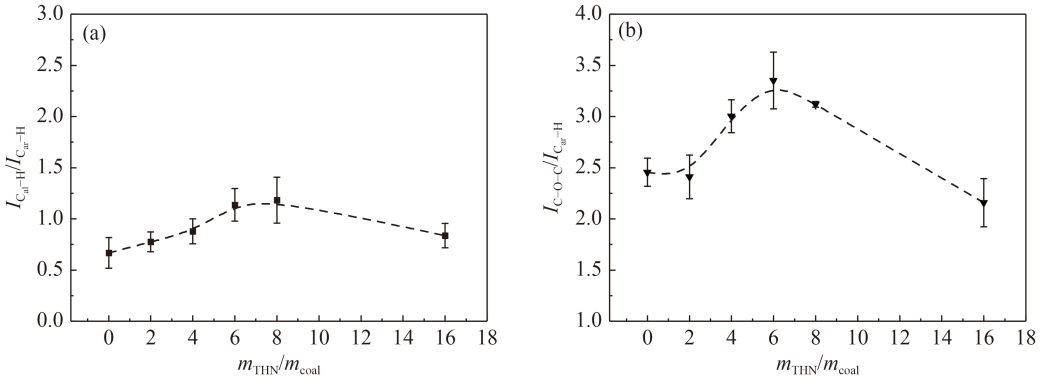

Fig. 9 Variation of the ratios of (a) $I_{C_{al}-H}/I_{C_{ar}-H}$ and (b) $I_{C-O-C}/I_{C_{ar}-H}$ with the ratio of tetralin to coal.

induced activation in the pyrolysis process of the side chain. Thus, the ratio of C_{al}–H was reduced.

As indicated in Fig. 9(b), the trend is an increase first, then a decrease with the addition of tetralin. The peak value appeared when m_{THN}/m_{coal} was 6. In general, raw coal contained some ether bonds, but the condensation process would also lead to the formation of ether bonds. However, it only had a slightly decreasing trend when the ratio of m_{THN}/m_{coal} increased from 0 to 2, and later increased significantly when m_{THN}/m_{coal} was greater than 2. This result indicates that the tetralin can hinder the cleavage of the C–O–C bond during the conversion. Combined with the DFT calculations, when the amount of tetralin increased, the radical fragments generated by coal pyrolysis were stabilized by tetralin, thus losing the ability to induce C–O–C bond cleavage. In the transformation process, C–O–C tended to increase with an increase in the proportion of tetralin. However, more H radicals were generated when m_{THN}/m_{coal} gradually increased. The H radicals acted as inducers with higher activity to induce the breaking of the C–O–C chemical bond. Therefore, with the increasing proportion of tetralin, both the C_{ar}–H and C–O–C bonds were transformed by the induction process of H radicals in the system. That is why the trend of Fig. 9 is both going down with the increase of the proportion of tetralin. The energy barrier required to induce toluene to release methyl was 252.3 kJ·mol^{-1} (free energy barrier, calculated by Gaussian 09), which is greater than 174.7 kJ·mol^{-1} in Fig. 3 and 236.1 kJ·mol^{-1} in Fig. 6. Therefore, the variation range of $I_{C_{al}-H}/I_{C_{ar}-H}$ is much smaller than that of $I_{C-O-C}/I_{C_{ar}-H}$, mainly because C_{ar}–C_{al} is more difficult to be induced by H radicals.

In addition, FTIR profiles of solid products produced by Series 2 was shown in Fig. S7 (cf. ESM). And the results were very similar to those in Series 1. Both $I_{C_{al}-H}/I_{C_{ar}-H}$ and $I_{C-O-C}/I_{C_{ar}-H}$ increased first and then decreased with the addition of tetralin. The difference of $I_{C_{al}-H}/I_{C_{ar}-H}$ between the two series was small. However, there were significant differences in $I_{C-O-C}/I_{C_{ar}-H}$ between these two series, which indicates that the existence of C–O–C was mainly generated at higher temperatures. But the newly formed C–O–C had higher BDE to break these C–O–C bonds. When m_{THN}/m_{coal} was less than 6, the increase in C–O–C was primarily due to the lessening of the coal radical radicals. When m_{THN}/m_{coal} was greater than 6, C–O–C production decreased due to the presence of H radicals with the increasing proportion of tetralin, which was consistent with the mechanism previously discussed.

3.5.3 EPR spectral analysis of radicals

The mechanism of the direct coal liquefaction is following the radical mechanism, which can be detected by the EPR instruments. According to the EPR spectral peak area corresponding to radical's content [40], the EPR signal in the solid products with different proportions of tetralin showed that the concentration of radicals gradually weakened with an increase in $m_{THN}/m_{coal,}$ as shown in Fig. 10. When m_{THN}/m_{coal} was 2, the accumulated content of radicals in solid products was apparent from Series 1 to 2. The results showed that the addition of tetralin decreased the condensation. When the m_{THN}/m_{coal} was increased to 4, the radical content in the product did not increase. Compared with the products of Series 1, the condensation was restricted after $m_{THN}/m_{coal} \geqslant 4$, but there were still radicals difficult to annihilate in the solid product of Series 2. When the condensation occurred, the coking reaction led to the pore contraction of the macromolecule reactant, and the tetralin was unable to contact the broken chemical bond, thus intensifying the condensation process [35]. The distribution of products, particularly the formation of heavy-molecular product, controlled by the addition of tetralin was relatively limited. Moreover, it was still challenging to stop the occurrence of this phenomenon when the ratio of tetralin increased.

4 Conclusions

H radicals formed from hydrogen-donor solvent in lignite hydrogenolysis would primarily be stabilized coal radical

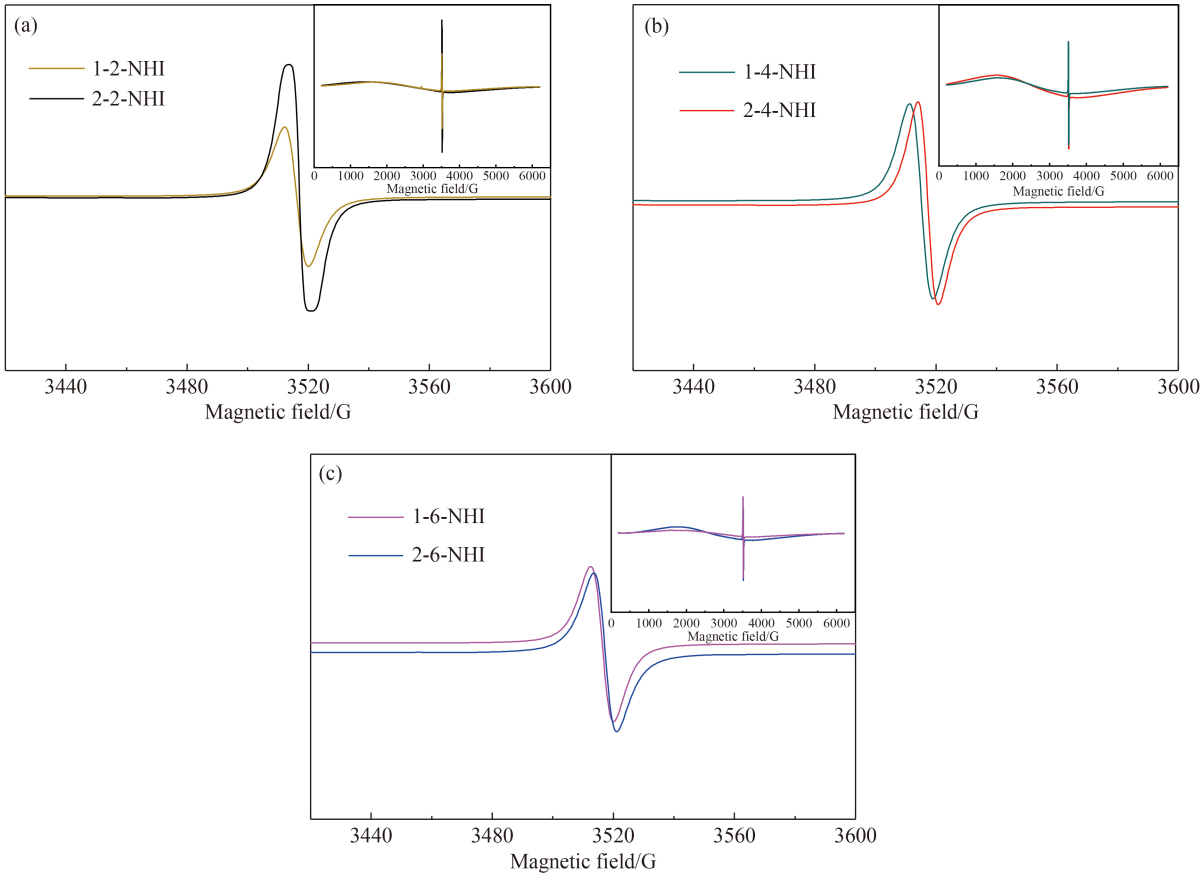

Fig. 10 EPR spectral analysis of NHI under different conditions: (a) 2, (b) 4, and (c) 6 times tetralin added at 400 and 450 °C, 40 min.

fragments. Most coal radical fragments were stabilized promptly as the proportion of hydrogen-donor solvents increased consecutively, and more hydrogen-donor solvents would be involved in the induction reaction. When the addition amount of hydrogen-donor solvent was low, the pyrolysis was mainly induced by coal radical fragments. Similarly, when the proportion of hydrogen-donor solvent increases, H radicals produced in the secondary hydrogen-supply process are implicated in the induction process, thereby simplifying the strong chemical bonds cleavage. Furthermore, the induction ability of H radical is more remarkable than that of benzyl radical.

A sequence dehydrogenation mechanism of hydrogen-donor solvent combining hydrogen abstraction reaction and self-dissociation of hydrogen supply solvent radicals is proposed. Furthermore, induced pyrolysis by the H radical produced after self-dissociation is investigated. Combining these two aspects forms the synergistic mechanism of hydrogen supply and hydrogenolysis of hydrogen-donor solvent. DFT calculations and experimental results of the transformation of hydroxyl groups and ether bonds both followed the same radical mechanism for lignite hydrogenolysis. This study elaborated on the hydrogenolysis mechanism of coal and the contribution of hydrogen-donor solvents. It will serve as a reference for the directional transformation of related functional groups.

Acknowledgements The authors are grateful to the National Natural Science Foundation of China (Grant No. 22038008) and the 2030 Major Project Pilot Project from CHN Energy, China (Grant No. GJNY2030XDXM-19-13,2) for the financial support.

Electronic Supplementary Material Supplementary material is available in the online version of this article at https://dx.doi.org/10.1007/s11705-022-2186-7 and is accessible for authorized users.

References

1. Vasireddy S, Morreale B, Cugini A, Song C S, Spivey J J. Clean liquid fuels from direct coal liquefaction: chemistry, catalysis, technological status and challenges. Energy & Environmental Science, 2011, 4(2): 311–345
2. Li W Y, Li W, Feng J. An overview on issues for lignite direct liquefaction. Journal of the China Coal Society, 2020, 45(1): 414–423 (in Chinese)
3. Chen Z, Xie J, Liu Q, Wang H, Gao S, Shi L, Liu Z. Characterization of direct coal liquefaction catalysts by their sulfidation behavior and tetralin dehydrogenation activity. Journal of the Energy Institute, 2019, 92(4): 1213–1222
4. Dorrestijn E, Laarhoven L J J, Arends I W C E, Mulder P. The occurrence and reactivity of phenoxyl linkages in lignin and low rank coal. Journal of Analytical and Applied Pyrolysis, 2000, 54(1–2): 153–192
5. Wei X Y, Ogata E, Qin Z H, Liu J Z, Zong Z M, Shen K, Zhou S

L, Li H Q. Advances in the study of hydrogen transfer to model compounds for coal liquefaction. Fuel Processing Technology, 2000, 62(2–3): 103–107
6. Barraza J, Coley Silva E, Piñeres J. Effect of temperature, solvent/coal ratio and beneficiation on conversion and product distribution from direct coal liquefaction. Fuel, 2016, 172: 153–159
7. Wang X B, Fan H H, Xie Z Z, Li W Y. Further discussion on the mechanism of hydrogen transfer in direct coal liquefaction. Catalysis Today, 2021, 374: 185–191
8. Yan J C, Bai Z Q, Bai J, Li W. Chemical structure and reactivity alterations of brown coals during thermal treatment with aromatic solvents. Fuel Processing Technology, 2015, 137: 117–123
9. Niu B, Jin L J, Li Y, Shi Z W, Hu H Q. Isotope analysis for understanding the hydrogen transfer mechanism in direct liquefaction of Bulianta coal. Fuel, 2017, 203: 82–89
10. Hou R R, Pang K L, Bai Z Q, Feng Z H, Ye D H, Guo Z X, Kong L X, Bai J, Li W. Study on carboxyl groups in direct liquefaction of lignite: conjoint analysis of theoretical calculations and experimental methods. Fuel, 2021, 286: 119298
11. Hou R R, Bai Z Q, Zheng H Y, Feng Z H, Ye D H, Guo Z X, Kong L X, Bai J, Li W. Behaviors of hydrogen bonds formed by lignite and aromatic solvents in direct coal liquefaction: combination analysis of density functional theory and experimental methods. Fuel, 2020, 265: 117011
12. Hao P, Bai Z Q, Hou R R, Xu J L, Bai J, Guo Z X, Kong L X, Li W. Effect of solvent and atmosphere on product distribution, hydrogen consumption and coal structural change during preheating stage in direct coal liquefaction. Fuel, 2018, 211: 783–788
13. Robinson K. Reaction engineering of direct coal liquefaction. Energies, 2009, 2(4): 976–1006
14. Grandy D W, Petrakis L E. investigation of free radicals in solvent-refined-coal materials. Fuel, 1979, 58(3): 239–240
15. Petrakis L, Grandy D W. Free radicals in coals and coal conversion. 2. Effect of liquefaction processing conditions on the formation and quenching of coal free radicals. Fuel, 1980, 59(4): 227–232
16. Petrakis L, Grandy D W. Free radicals in coal and coal conversions. 6. Effects of liquefaction process variables on the in-situ observation of free radicals. Fuel, 1981, 60(11): 1017–1021
17. Petrakis L, Jones G L, Grandy D W, King A B. Free radicals in coal and coal conversions. 10. Kinetics and reaction pathways in hydroliquefaction. Fuel, 1983, 62(6): 681–689
18. Kim K H, Bai X, Brown R C. Pyrolysis mechanisms of methoxy substituted α-O-4 lignin dimeric model compounds and detection of free radicals using electron paramagnetic resonance analysis. Journal of Analytical and Applied Pyrolysis, 2014, 110: 254–263
19. Chen Z Z, Zhang X R, Liu Z Y, Liu Q Y, Xu T. Quantification of reactive intermediate radicals and their induction effect during pyrolysis of two *n*-alkylbenzenes. Fuel Processing Technology, 2018, 178: 126–132
20. Guo X, Liu Z, Xiao Y, Xu X, Xue X, Liu Q. The Boltzmann-Monte-Carlo-Percolation (BMCP) model on pyrolysis of coal: the volatiles' reactions. Fuel, 2018, 230: 18–26
21. Bi S S, Guo X J, Wang B, Xu X, Zhao L F, Liu Q Y. A DFT simulation on induction reactions involved radicals during pyrolysis of heavy organics. Journal of Fuel Chemistry & Technology, 2021, 49(5): 684–693
22. Han Y, Jiang D, Zhang J, Li W, Gan Z, Gu J. Development, applications and challenges of ReaxFF reactive force field in molecular simulations. Frontiers of Chemical Science and Engineering, 2016, 10(1): 16–38
23. Yan B, Zhang G, Gao P, Li H, Ren S, Wu W. Dissolution behavior of hydrogen in the model recycle solvent of mild direct coal liquefaction. Fuel Processing Technology, 2021, 223: 106982
24. Bai J K, Zhang X B, Li W, Wang X B, Du Z Y, Li W Y. Rate constant of hydrogen transfer from H-donor solvents to coal radicals. Fuel, 2022, 318: 12361
25. Zhang X R, Liu Z Y, Chen Z Z, Xu T, Liu Q Y. Bond cleavage and reactive radical intermediates in heavy tar thermal cracking. Fuel, 2018, 233: 420–426
26. Zhu C, Cao J P, Feng X B, Zhao X Y, Yang Z, Li J, Zhao M, Zhao Y P, Bai H C. Theoretical insight into the hydrogenolysis mechanism of lignin dimer compounds based on experiments. Renewable Energy, 2021, 163: 1831–1837
27. Li L, Fan H J, Hu H Q. A theoretical study on bond dissociation enthalpies of coal based model compounds. Fuel, 2015, 153: 70–77
28. Xie T, Cao J P, Zhu C, Zhao X Y, Zhao M, Zhao Y P, Wei X Y. Selective cleavage of C–O bond in benzyl phenyl ether over Pd/AC at room temperature. Fuel Processing Technology, 2019, 188: 190–196
29. Kong L, Li G, Jin L, Hu H. Pyrolysis behaviors of two coal-related model compounds on a fixed-bed reactor. Fuel Processing Technology, 2015, 129: 113–119
30. Li W, Feng J, Feng M M, Wang X B, Li W Y. Distribution, migration and transformation of oxygen during the hydrogenation reaction of lignite. Journal of the China Coal Society, 2021, 46(4): 1080–1087 (in Chinese)
31. Gaussian 09, Revision A.02. Wallingford CT: Gaussian, Inc., 2016
32. Zhao Y, Truhlar D G. The M06 suite of density functionals for main group thermochemistry, thermochemical kinetics, noncovalent interactions, excited states, and transition elements: two new functionals and systematic testing of four M06-class functionals and 12 other functionals. Theoretical Chemistry Accounts, 2007, 120(1–3): 215–241
33. Biczysko M, Panek P, Scalmani G, Bloino J, Barone V. Harmonic and anharmonic vibrational frequency calculations with the double-hybrid B2PLYP method: analytic second derivatives and benchmark studies. Journal of Chemical Theory and Computation, 2010, 6(7): 2115–2125
34. Hemelsoet K, Speybroeck V V, Waroquier M. Bond dissociation enthalpies of large aromatic carbon-centered radicals. Journal of Physical Chemistry A, 2008, 112(51): 13566–13573
35. Liang S, Hou Y, Wu W, Li H, He Z, Ren S. Residues characteristics and structural evolution of Naomaohu coal during a mild direct liquefaction process. Fuel Processing Technology, 2021, 215: 106753
36. Feng J, Li W Y, Xie K C. Research on coal structure using FT-IR.

Journal of China University of Mining and Technology, 2002, 31(5): 362–366

37. Shui H, Ma X, Yang L, Shui T, Pan C, Wang Z, Lei Z, Ren S, Kang S, Xu C C. Thermolysis of biomass-related model compounds and its promotion on the thermal dissolution of coal. Journal of the Energy Institute, 2017, 90(3): 418–423
38. Zhu C, Ding S, Hojo H, Einaga H. Controlling diphenyl ether hydrogenolysis selectivity by tuning the Pt support and H-donors under mild conditions. ACS Catalysis, 2021, 11(20): 12661–12672
39. Trewhella M J, Grint A. Condensation of phenolic groups during coal liquefaction model compound studies. Fuel, 1988, 67(8): 1135–1138
40. Liu J, Jiang X, Shen J, Zhang H. Chemical properties of superfine pulverized coal particles. Part 1. Electron paramagnetic resonance analysis of free radical characteristics. Advanced Powder Technology, 2014, 25(3): 916–925